Hindawi Publishing Corporation
EURASIP Journal on Wireless Communications and Networking
Volume 2010, Article ID 526429, 8 pages
doi:10.1155/2010/526429

Research Article

Cyclostationarity Detectors for Cognitive Radio: Architectural Tradeoffs

Dominique Noguet, Lionel Biard, and Marc Laugeois

CEA-LETI-MINATEC, 17 rue des Martyrs, 38054 Grenoble cedex 9, France

Correspondence should be addressed to Dominique Noguet, dominique.noguet@cea.fr

Received 17 November 2009; Revised 25 February 2010; Accepted 15 July 2010

Academic Editor: Danijela Cabric

Cyclostationarity detectors have been studied in the past few years as an efficient means for signal detection under low-SNR conditions. On the other hand, some knowledge about the signal is needed at the detector. This is typically the case in Cognitive Radio spectrum secondary usage, where the primary system is known. This paper focuses on two hardware architectures of cyclostationarity detectors for OFDM signals. The first architecture aims at secondary ISM band use, considering IEEE802.11a/g as the primary system. In this scenario, low latency is required. The second architecture targets TV band secondary usage, where DVB-T signals must be detected at very low SNR. The paper focuses on the architectural tradeoffs that the designer has to face, and how his/her choices will influence either performance or complexity. Hardware complexity evaluation on FPGA is provided for detectors that have been tested in the laboratory under real conditions.

1. Introduction

Recently, there has been a growing interest in signal detection in the context of Cognitive Radio [1], and more specifically in that of opportunistic radio, where secondary Cognitive Radio Networks (CRNs) can be operated over frequency bands allocated to some primary system in so far as this primary system is absent or, in a more general case, whenever harmful interference with primary systems can be avoided. In most cases, the presence of the primary system is assessed through direct detection of its communication signal, although beaconing is sometimes considered [2]. Thus, in many situations, the primary system detection problem is transposed to the problem of detecting a communication signal in the presence of noise. Surveys of signal detection in the context of spectrum sensing have been proposed in the literature [3, 4]. These detectors operate according to the *a priori* knowledge they have about the signal and the model of this signal. Telecommunication signals are modulated by sine wave carriers, pulse trains, repeated spreading, hopping sequences, or exhibit cyclic prefixes. Thus, these signals are characterized by the fact that their momentum (mean, autocorrelation, etc.) exhibits periodicity. This built-in periodicity, which of course is not present in noise, can be exploited to detect signals in the presence of noise even at a low Signal-to-Noise Ratio (SNR) [5]. Using this model, the signal detection process becomes a test for presence of cyclostationary characteristics of the tested signal [6–8].

Many scenarios have been investigated in the context of CRN over the past years. The two most likely to occur in the short term are, on the one hand, the unlicensed usage of TV bands and, on the other hand, the opportunistic use of unlicensed bands by nonlegacy secondary systems. The first scenario, often referred to as the TV White Space (TVWS) scenario, was made possible by the FCC in the US in 2008, with some restrictions which include high-sensitivity requirements for primary user detection [9]. In the context of this scenario, standardization has been very active, especially under the IEEE802.22 banner [10]. Industry fora, like the White Space Coalition, have given more momentum to this option. The second scenario is, for obvious regulatory reasons, the first that can be practically experimented and used [11].

In this context, implementation of blind cyclostationarity detectors has been proposed. In [12], a detector based on Cyclostationary Spectrum Density (CSD) is suggested. The CSD theoretically makes it possible to explore the presence of cyclic frequencies for any autocorrelation lag at any frequency (also referred to as 2D CSD). However, the comprehensive 2D CSD is never implemented in practice due to its huge implementation cost. To sort out this issue, 1D CSDs are preferred to limit implementation cost. The CSD can be performed on the time domain autocorrelation [13, 14], or through the analysis of signal periodicity redundancy in the frequency domain [15]. In both cases however, a large FFT operator (512 to 2048) needs to be implemented, leading to significant hardware complexity. The approach described hereafter goes one step further in narrowing down the CSD domain. Indeed, in both scenarios of interest, the primary systems (which are the ones requiring the highest detection sensitivity) are known. Therefore, analysis of the primary signal nature helps narrow down the CSD search to very specific cyclic frequencies, thereby avoiding implementation of a large FFT.

However, when the CSD is narrowed down, the algorithm becomes more specific to the signal to detect. For this reason, this paper will analyze two different implementation options depending on the aforementioned scenarios. The main reason justifying different types of implementation in the WiFI and TVWS scenarios is the sensitivity level required in each case. In the case of TVWS, the guarantee that secondary CRN will not interfere with licensed systems (TV, microphones) leads to high-sensitivity requirements. On the other hand, unlicensed band networks, such as IEEE802.11x, have lighter coexistence constraints. These specific requirements lead to architectural tradeoffs which are examined in this paper. First, the principle of prefix-based cyclostationarity detection will be recapped. Then, the two aforementioned scenarios will be analyzed by pinpointing their impact on the sensor requirement. Considering these requirements, two hardware implementation architectures will be described and evaluated. These approaches will be compared and discussed before concluding the paper.

2. Cyclostationarity Detector for OFDM Signal

In both scenarios considered in this paper, in the primary system—DVB-T broadcast system on the one hand, IEEE802.11a/g networks on the other—the signal is modulated using Orthogonal Frequency Digital Multiplexing (OFDM); see, for example, [16]. The OFDM signal is a compound signal consisting of multiple frequency carriers, also called subcarriers or tones, that are each modulated in phase or in phase and amplitude. From a practical outlook, the modulated tones are multiplexed at the transmitter using an inverse FFT. Conversely, the subcarriers are demultiplexed at the receiver end by an FFT. The size of the FFT N, which defines that of the OFDM symbols, depends on the system. In the case of IEEE802.11a/g systems, 64 subcarriers are used whereas the DVB-T signal uses 1024, 2048, 4096, or 8192 tones. In order to avoid intersymbol interference, a Guard Interval (GI) is introduced. In the case of OFDM, this GI is designed as a copy of the last samples of the OFDM symbol. This approach provides the symbol with a cyclic nature which simplifies the receiver. For this reason, this D long GI is called the Cyclic Prefix (CP).

Let us now consider the autocorrelation of this signal,

$$R_y(u,m) = E\big(y(u+m)\cdot y^*(u)\big). \tag{1}$$

Under the condition that all subcarriers are used, the autocorrelation of an OFDM signal is written as [17]

$$\begin{aligned} R_y(u,m) = {} & R_y(u,0)\delta(m) + R_y(u,N)\delta(m-N) \\ & + R_y(u,-N)\delta(m+N). \end{aligned} \tag{2}$$

The first term corresponds to the energy of the signal. Energy detectors, which analyze this term only, provide poor performance at low SNR. Therefore, we focus on the two other terms, which stem from the repetition of the cyclic prefix present at the beginning and the end of each symbol. It can be shown that the term $R_y(u,N)$ is a periodic function of u [8] which characterizes the signal y. $R_y(u,N)$ has a period of $\alpha^{-1} = N + D$. This cyclostationary nature of the signal is illustrated in Figure 1.

Thus, $R_y(u,N)$ can be written as a Fourier series [5]:

$$R_y(u,N) = R_y^0(N) + \sum_{k=-\alpha^{-1}/2,\,k\neq 0}^{k=\alpha^{-1}/2-1} R_y^{k\alpha}(N) e^{2j\pi k\alpha u}. \tag{3}$$

In (3), each Fourier coefficient $R_y^{k\alpha}(N)$ is the cyclic correlation at frequency $k\alpha$ at time lag N. This term is also written as

$$R_y^{k\alpha}(N) = \lim_{U\to\infty}\frac{1}{U}\sum_{u=0}^{u=U-1} E\big(y(u+N)y^*(u)\big)\cdot e^{-2j\pi k\alpha u}, \tag{4}$$

which can be estimated as follows:

$$\hat{R}_y^{k\alpha}(N) = \frac{1}{U}\sum_{u=0}^{u=U-1} y(u+N)y^*(u)\cdot e^{-2j\pi k\alpha u}. \tag{5}$$

The basic idea behind the cyclostationarity detector is to analyze this Fourier decomposition and assess the presence of the signal by setting a cost function related to one [18] or more [19] of these cyclic frequencies. This cost function is compared to some reference value. Several papers related to this algorithm have been proposed in the literature [17, 19–21]. They mainly differ in the way the harmonics are considered. In this paper, we consider the cost function suggested in [17]. By introducing the oversampling rate of T_c/T_e and by considering N_b harmonics, this cost function can be derived from (5) as follows:

$$J_{y,N}(N_b) = \sum_{k=-N_b}^{N_b}\left|\sum_{u=0}^{U-1} y\left((u+N)\frac{T_c}{T_e}\right)y^*\left(u\frac{T_c}{T_e}\right)e^{(-2i\pi ku/N+D)(T_c/T_e)}\right|^2. \tag{6}$$

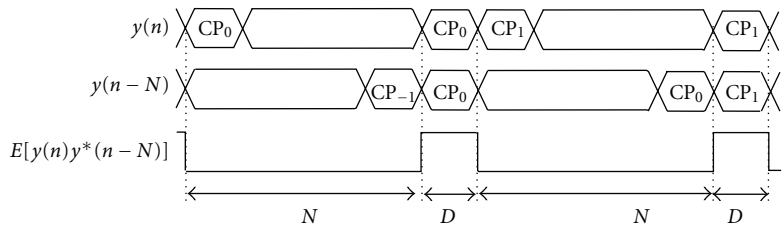

Figure 1: Ideal autocorrelation signal of an OFDM symbol burst.

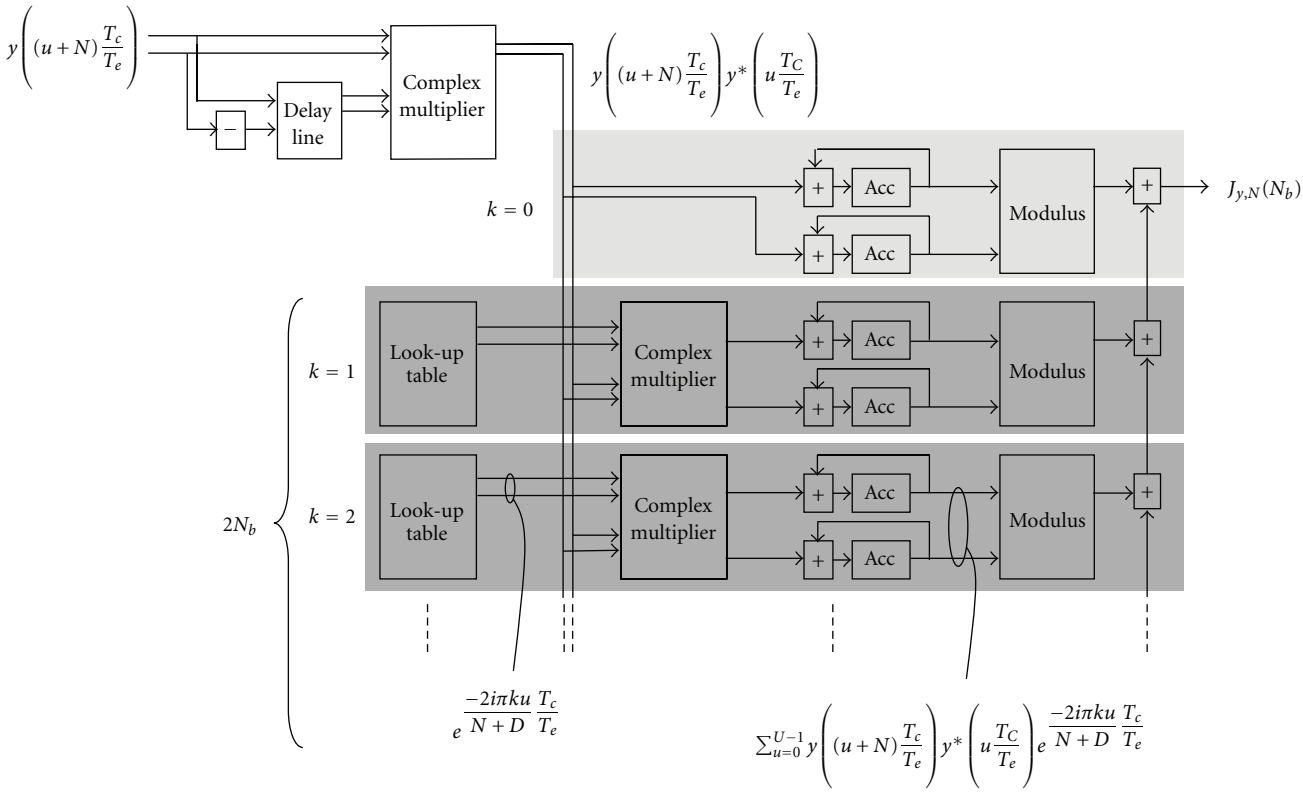

Figure 2: Cyclostationarity detector for WiFi signals.

It can be observed that the cost function is only built upon $R_y^{k\alpha}(N)$ while $R_y^{-k\alpha}(-N)$ is omitted. Indeed, it is fairly easy to prove that for all k, $\hat{R}_y^{k\alpha}(N) = \hat{R}_y^{-k\alpha}(-N)^*$ (where $*$ denotes the complex conjugation).

3. Cyclostationarity Detector Architecture for WiFi Signals

The cyclostationarity detector for IEEE802.11a/g signals is specified considering the scenario presented in [22]. In this scenario, the detector is used to check the presence of WiFi signals in order to trigger data transmission from a secondary system which is completely independent from the primary system (no messaging exchanged, no synchronization performed). Besides, in order to achieve the highest spectrum efficiency, the secondary system is expected to exploit time gaps (opportunities) in the time domain rather than to leave the channel to find a vacant one. Although this strategy may lead to some collisions, it is found acceptable due to the nature of the primary (unlicensed system) and in so far as the impact is not significant at application level [22].

Focusing on the design of the cyclostationarity detector, this scenario leads to the requirements of a low-latency detector. Detector latency directly impacts the duration of the time gaps that will be exploited by the secondary system. When the primary system is bursty, which is the typical nature of WiFi traffic, latency should be far shorter than the gaps between two consecutive bursts. The need for low latency calls for a parallel approach in which the Fourier coefficients are computed at the same time. Such a structure is described in Figure 2.

This architecture is directly derived from (6). The top left corner block computes one single observation of the

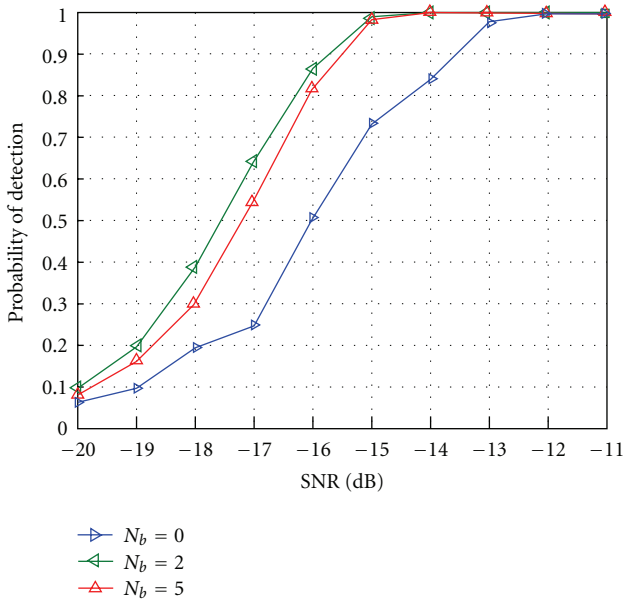

Figure 3: Influence of N_b.

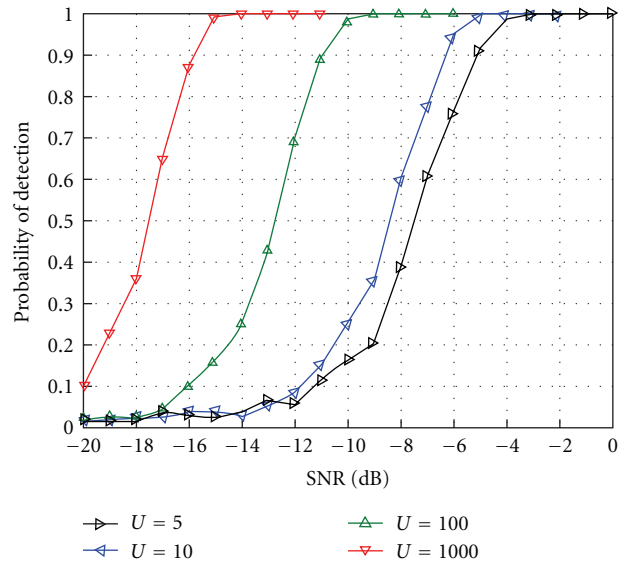

Figure 4: Influence of U (with $N_b = 2$).

autocorrelation function. Each grey block then computes the Fourier coefficients in parallel. Each of these branches is accumulated over the observation time U before being aggregated by the sum blocks on the right of the figure.

The first point to consider when designing a parallel architecture is to analyze how many branches need to be instantiated. In other words, how the cyclostationary detector performs according to N_b. For this purpose, the probability of detection is computed as a function of the SNR under AWGN conditions for various N_b values. Other parameters are kept constant. For instance U is set to a large value ($U = 1000$). The results obtained are provided in Figure 3. For Figures 3–6, 1000 independent iterations have been carried out to build the curve.

Selecting $N_b = 0$ corresponds to considering the fundamental frequency only, which is equivalent to performing energy detection. Detector performance is maximized for a small N_b value, which implies that performance can be maximized for a limited hardware complexity. Aggregating harmonics still further causes performance to decrease since high harmonics, of low amplitude, are strongly impacted by noise. This shows that performance can be optimized with respect to N_b while preserving a limited hardware complexity.

Another important parameter for the detector is the size of the integration window U (where U denotes the number of OFDM symbols considered for integration). Although this parameter has a more limited impact on hardware complexity (only the accumulators are slightly larger), U has a strong influence on latency, another major requirement in the scenario. As expected, increasing U does indeed improve performance significantly as shown in Figure 4.

Limiting detector latency while preserving performance of long observation time is possible by trading U against T_c/T_e ($F_e = 1/T_e = 20$ MHz). Oversampling is expected to have a similar influence on performance in that it increases U, except for the fact that T_c/T_e cannot be reasonably increased to a similar extent to U. Therefore, whenever latency is not critical, increasing U should be considered. Besides, increasing T_c/T_e directly impacts the length of the delay line of the correlator, as well as the look-up tables used for storage of the sine waveforms, whereas U had only a slight impact on the complexity of the accumulators in each branch. Thus, priority should be given to increasing U in so far as detector latency fits into the latency specification. In the case of the WiFi detector, 5 OFDM symbols correspond to a latency of 20 μs. Additional performance can then be ensured by a reasonable increase in T_c/T_e to limit the additional complexity drawback. Figure 5 shows the influence of T_c/T_e.

Finally, the last parameter that needs to be determined is W, the width of the binary word representing the I/Q input data. Assuming that the full dynamic range is preserved throughout the architecture, it is obvious that this parameter will significantly impact hardware complexity. However, the impact on detector performance is less obvious, and some simulations must be quantified. These simulation results are provided in Figure 6.

Figure 6 shows that near optimal performance can be obtained where $W = 4$. However, to preserve some additional margin, a value of 8 is preferred, with rescaling after each macro block to guarantee a good performance/complexity tradeoff. With these parameters, detector overall latency has been measured at 40.5 μs.

Finally, the complexity of detector hardware implementation is determined on a Xilinx Virtex 4 target technology using the ISE XST synthesis tool. Results are provided in Table 1 when the following parameter values are considered: $N = 64$, $D = 16$, $U = 5$, $N_b = 2$, $T_c/T_e = 1$, and $W = 4$.

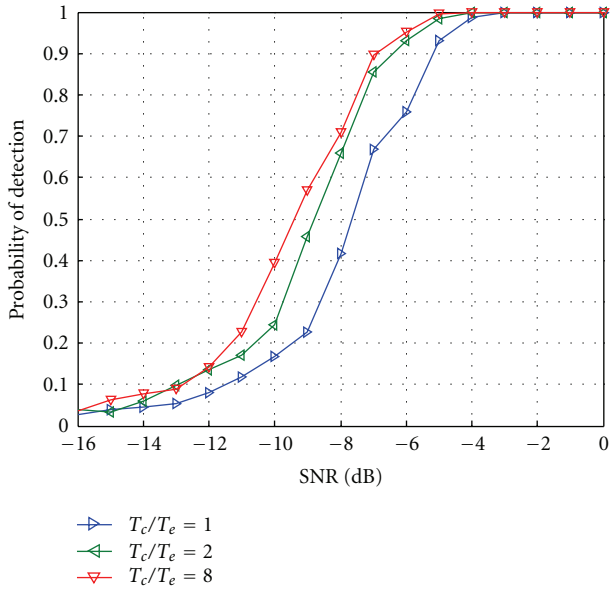

Figure 5: Influence of T_c/T_e ($N = 64$, $D = 16$, $U = 5$, $N_b = 2$).

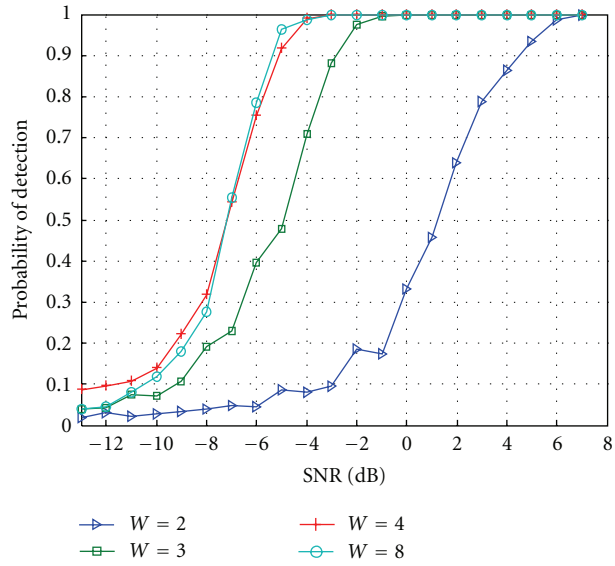

Figure 6: Influence of W ($N = 64$, $D = 16$, $U = 5$, $N_b = 2$, $T_c/T_e = 1$)

4. Cyclostationarity Detector Architecture for DVB-T Signals

In the same way as IEEE802.11a/g, the physical layer of DVB-T is based on an OFDM modulation. However, some key elements differ from WiFi systems. First, the DVB-T standard defines four FFT sizes: $N = 1024$, 2048, 4096, or 8192, and $F_e = 8$ MHz. The cyclic prefix over FFT size ratio D/N can also vary: 1/32, 1/16, 1/8, and 1/4. However, in practice, implementation considers a smaller set of parameters depending on the country.

For instance, in France, the set of parameters used is $N = 8192$, $D/N = 1/32$. Another key difference, which will be exploited in the architecture design, stems from the broadcast nature of the DVB-T signal. This means that detector sensitivity can be increased significantly by very long integration time which cannot be considered in the case of short signal bursts occurring in WiFi. This is, of course, a relevant feature since sensitivity requirements for primary user detection are very demanding (typically SNR = −10 dB, to which an additional margin for detector Noise Figure must be added [23]).

Another point derived from the broadcast nature of the signal is the way the reference signal used to define the decision threshold is computed. When undertaking this calibration phase, the secondary system needs to consider a reference value which is independent from signal presence. When considering long (ideally infinite) integration time, the autocorrelation function $R_y(u, N)$ defined in Section 2 tends to a rectangular signal as depicted in Figure 1, the cyclic ratio of which is $D/(N + D)$. In this case, the Fourier coefficient is written as

$$R_y^{k\alpha}(N) = \frac{A}{2\pi \cdot k}\left[\sin\frac{2\pi \cdot k \cdot D}{N+D} + j\left(1 - \cos\frac{2\pi \cdot k \cdot D}{N+D}\right)\right]. \quad (7)$$

Table 1: Complexity evaluation of the WiFi detector.

Complexity			Latency
Slices	RAM	Mult	
1960	0	35	40.5 μs

Each coefficient power is given by

$$\left|R_y^0\right|^2 = \left(\frac{A \cdot D}{N+D}\right)^2, \quad k = 0,$$
$$\left|R_y^{k\alpha}\right|^2 = 2\left(\frac{A}{2\pi k}\right)^2\left(1 - \cos\frac{2\pi \cdot k \cdot D}{N+D}\right), \quad k \neq 0. \quad (8)$$

It is obvious from (8) that $R_y^{k\alpha}(N) = 0$ whenever $kD/(N+D)$ is an integer value. This holds for instance when

$$k = \frac{N}{D} + 1. \quad (9)$$

Figure 7 plots the Fourier coefficients of a rectangular signal when $N/D = 32$.

It can therefore be concluded that Fourier harmonic 33 is not impacted by the presence of the signal and can thus be used for calibration purposes to define the reference noise level. As a comparison, calibration based on input power computation (i.e., $(1/U)\sum_{u=0}^{U-1}|y(u)|^2$) is not relevant as this estimator is strongly impacted by the presence of the signal. When considering the first 4 harmonics $[-3; +3]$, a decision variable V can be expressed as follows:

$$V = \frac{2}{7}\frac{\sum_{i=-3}^{3}|h_i|^2}{|h_{-33}|^2 + |h_{33}|^2}. \quad (10)$$

Of course, this technique holds for infinite integration time to guarantee the rectangular shape of the autocorrelation

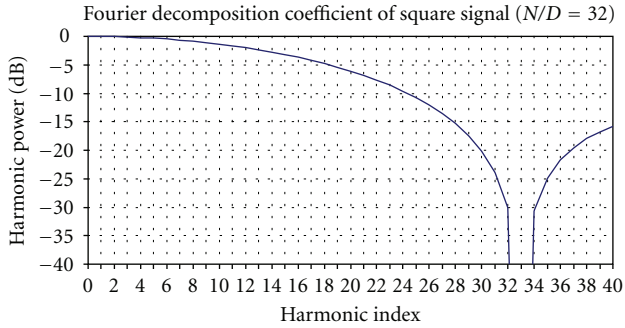

Figure 7: Fourier coefficient values for $N/D = 32$.

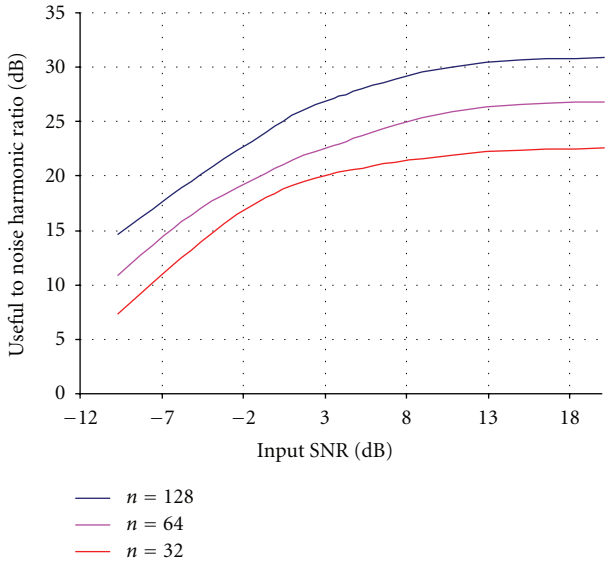

Figure 8: Detection threshold according to the input SNR.

estimator (Figure 1). Whenever a finite integration is performed, the convergence of the integrator needs to be considered. The integrator is a first order IIR filter, the z transform of which is given by

$$H(z) = \frac{1}{n}\frac{1}{1-((n-1)/n)z^{-N}}, \tag{11}$$

where n can be tuned to adjust the raising time of the filter. Indeed, the indicial response of the filter is given by

$$s_{\text{ind}}(k) = 1 - \left(\frac{n-1}{n}\right)^{k} \quad (k \geq 0). \tag{12}$$

The raising time k_r (in number of symbols) to reach 90% is then given by

$$k_r \leq \frac{2.3}{\ln(n/(n-1))} - 1 \leq k_r + 1. \tag{13}$$

Table 2: Complexity evaluation of the DVB-T detector.

Complexity			Latency
Slices	RAM blocks of 18 kbits	Mult	
1600	122	23	Depends on n

For large n values, the expression in (13) tends to $2.3n$. Estimator performance is increased by increasing the integration ability of the filter. This is, however, at the cost of long integration time. Thus, this approach is to be considered for "always on" kind of systems, such as DVB-T broadcast signals to guarantee reliable detection under low SNR-conditions.

Figure 8 shows the decision variable V as a function of the input SNR (under AWGN conditions) for several values of n. The area before the curve corresponds to a 0.5 detection probability and must be avoided. The aim of the curve is to show how increase in integration time impacts the performance of the detector for a given threshold value. For instance when an SNR of −7 dB is targeted and for a threshold set to 15, no detection is possible when considering $n = 32$. However, when n is set to 128, a reliable behavior is achieved. Setting n to 64 results in nonreliable decisions. From this graph, a trade-off between SNR detection condition and integration time can be set.

Detection and probability detection curves based on real signal measurements will be provided in a future paper. However, in order to evaluate a first implementation of the detector, parameter values used for the WiFi case were considered as an initial assumption. Finally, the cyclostationary detector hardware architecture for DVB-T is shown in Figure 9. First, the autocorrelation is computed on the I/Q complex samples. The IIR integrator then averages over a number of symbols tuned by setting the integration time parameter to achieve the required sensitivity. The supervisor, a Finite State Machine (FSM), then triggers the writing into a buffer that stores 8 k filter output samples (equivalent to the length of an OFDM symbol). Then, using a faster clock, the Fourier harmonics are computed sequentially. Unlike parallel computation over distinct instances in the architecture of Section 2, parallelism is achieved here using a faster clock and some control mechanisms provided by the FSM, even though latency constraints are not as critical as in the first case study. The sine generator computes sequentially the required sine function of the Fourier taps of interest. The Multiply ACcumulate (MAC) function enables the Fourier coefficient to be obtained for these taps. The sequence is as follows. First, the reference harmonics $\{-33; +33\}$ are generated to compute the noise reference power. Then, the harmonics of interest for the DVB-T signal $\{0; -1; +1; -2; +2; -3; +3\}$ are calculated. The power of each harmonic is summed up to obtain the cyclostationarity estimator value. Finally, the decision engine gives the final result by comparing the estimated value to the threshold value according to (10), which provides a hard decision output of the detector.

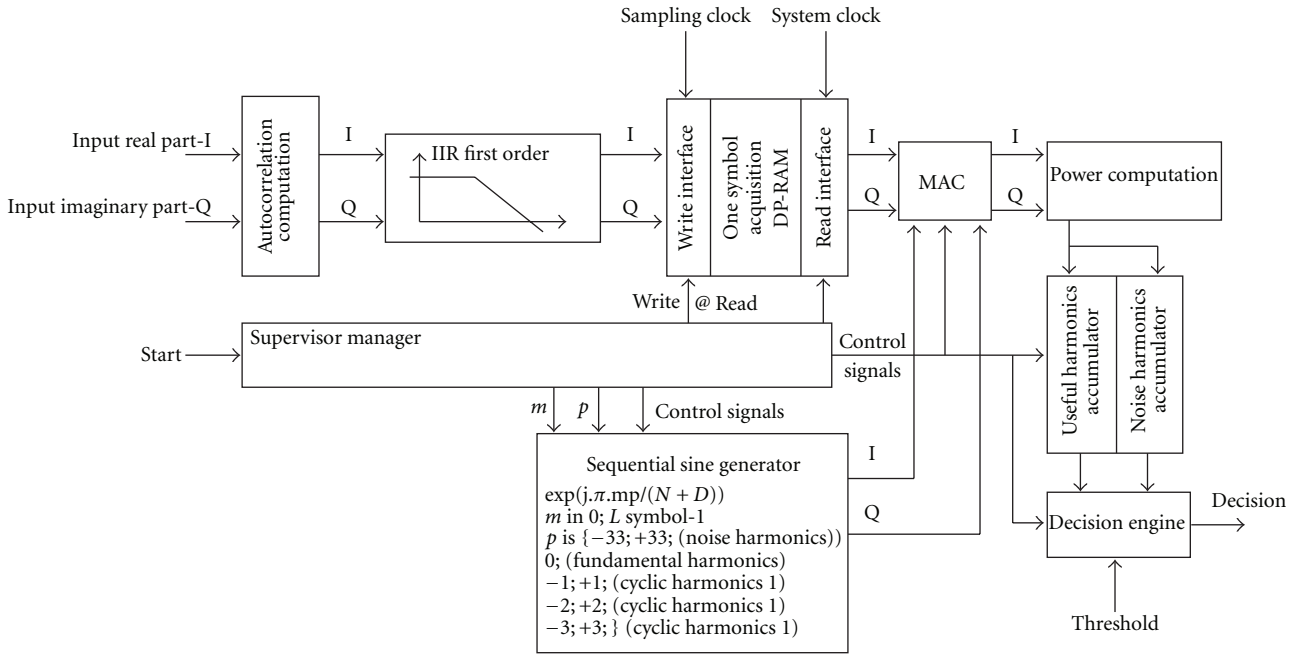

Figure 9: Cyclostationarity detector for DVB-T signals.

Finally, the complexity of detector hardware implementation is determined on a Xilinx Virtex 5 target technology using the ISE XST synthesis tool. Results are provided in Table 2.

5. Conclusion

This paper presents 2 cyclostationarity detectors targeting different scenarios. It is shown in the paper that selection of the scenario has a strong influence on architecture and its performance tradeoffs. First, when aiming at secondary usage of ISM bands with time leftover reuse, latency is the key parameter. With this architecture, latency as low as 40.5 μs was measured. Besides, the cyclostationary detectors of this paper outperform classical energy detectors in terms of probability of detection (e.g., Pd is increased by 0.4 where SNR = −17 dB in the WiFi case). This has led to a parallel design in which sensitivity is traded against low latency as collisions with the primary system may be tolerated. On the other hand, when considering secondary spectrum usage of licensed bands, collisions are not permitted and much attention must be paid to sensitivity. This is achieved through long integration time which relies on the assumption that the signal is either "always on" or absent. This assumption makes the second architecture ideally suited to broadcast signal detection (e.g., DVB-T), but would be inapplicable to the first scenario.

Acknowledgments

The authors would like to acknowledge the ORACLE European IST project of the 6th Framework Program and the French ANR INFOP project for supporting the work presented in this paper.

References

[1] J. Mitola, *Cognitive radio: an integrated agent architecture for software defined radio*, Ph.D. thesis, Royal Institute of Technology, Stockholm, Sweden, May 2000.

[2] L. Berlemann and S. Mangold, *Cognitive Radio and Dynamic Spectrum Access*, John Wiley & Sons, New York, NY, USA, 2009.

[3] A. Sahai and D. Cabric, "A tutorial on spectrum sensing: fundamental limits and practical challenges," in *Proceedings of the IEEE Symposium on New Frontiers in Dynamic Spectrum Access Networks (DySPAN '05)*, Baltimore, Md, USA, November 2005.

[4] D. Noguet et al., "Sensing techniques for cognitive radio—state of the art and trends," April 2009, http://grouper.ieee.org/groups/scc41/6/documents/white_papers/P1900.6_WhitePaper_Sensing_final.pdf.

[5] W. A. Gardner, *Statistical Spectral Analysis: A Nonprobabilistic Theory*, Prentice-Hall, Englewood Cliffs, NJ, USA, 1988.

[6] G. D. Živanović and W. A. Gardner, "Degrees of cyclostationarity and their application to signal detection and estimation," *Signal Processing*, vol. 22, no. 3, pp. 287–297, 1991.

[7] W. A. Gardner and C. M. Spooner, "Signal interception: performance advantages of cyclic-feature detectors," *IEEE Transactions on Communications*, vol. 40, no. 1, pp. 149–159, 1992.

[8] W. Gardner and A. William, *Cyclostationarity in Communications and Signal Processing*, IEEE Press, New York, NY, USA, 1994.

[9] "FCC adopts rules for unlicensed use of television white spaces," Official announcement of FCC, November 2008, http://www.fcc.gov/.

[10] IEEE 802.22, "Wireless Regional Area Networks ("WRANs")," http://www.ieee802.org/22/.

[11] L. Biard, D. Noguet, T. Gernandt, P. Marques, and A. Gameiro, "A hardware demonstrator of an opportunistic radio system using temporal opportunities," in *Proceedings of the 4th International Conference on Cognitive Radio Oriented Wireless Networks and Communications (CrownCom '09)*, pp. 1–6, Hanover, Germany, June 2009.

[12] Z. Ye, J. Grosspietsch, and G. Memik, "Spectrum sensing using cyclostationary spectrum density for cognitive radios," in *Proceedings of the IEEE Workshop on Signal Processing Systems*, Shanghai, China, October 2007.

[13] V. Turunen, M. Kosunen, A. Huttunen et al., "Implementation of cyclostationary feature detector for cognitive radios," in *Proceedings of the 4th International Conference on Cognitive Radio Oriented Wireless Networks and Communications (CrownCom '09)*, Hannover, Germany, June 2009.

[14] V. Turunen, M. Kosunen, S. Kallioinen, A. Parssinen, and J. Ryynanen, "Spectrum estimator and cyclostationary detector for cognitive radio," in *European Conference on Circuit Theory and Design (ECCTD '09)*, pp. 283–286, Antalya, Turkey, August 2009.

[15] Y. Tachwali, M. Chmeiseh, F. Basma, and H. H. Refai, "A frequency agile implementation for IEEE 802.22 using software defined radio platform," in *Proceedings of the IEEE Global Telecommunications Conference (GLOBECOM '08)*, pp. 3128–3133, New Orleans, La, USA, December 2008.

[16] R. Prasad, *OFDM for Wireless Communications Systems*, Artech House, Norwood, Mass, USA, 1999.

[17] P. Jallon, "A spread signals detection algorithm based on the second order statistics in semi-blind contexts," in *Proceedings of the 3rd International Conference on Cognitive Radio Oriented Wireless Networks and Communications (CrownCom '08)*, May 2008.

[18] A. V. Dandawaté and G. B. Giannakis, "Statistical tests for presence of cyclostationarity," *IEEE Transactions on Signal Processing*, vol. 42, no. 9, pp. 2355–2369, 1994.

[19] J. Lundén, V. Koivunen, A. Huttunen, and H. V. Poor, "Spectrum sensing in cognitive radios based on multiple cyclic frequencies," in *Proceedings of the 2nd International Conference on Cognitive Radio Oriented Wireless Networks and Communications (CrownCom '07)*, pp. 37–43, Orlando, Fla, USA, August 2007.

[20] M. Ghozzi, M. Dohler, F. Marx, and J. Palicot, "Cognitive radio: methods for detection of free bands," *Elsevier Science Journal*, vol. 7, pp. 794–805, 2006.

[21] A. Bouzegzi, P. Jallon, and P. Ciblat, "A second order statistics based algorithm for blind recognition of OFDM based systems," in *Proceedings of the IEEE Global Telecommunications Conference (GLOBECOM '08)*, pp. 3257–3261, December 2008.

[22] ORACLE D6.1 Deliverable, "Definition of test scenarios for the demonstrator," August 2007, http://www.ist-oracle.org/.

[23] S. Shellhammer, "Spectrum sensing in IEEE802.22," in *Proceedings of the 1st IAPR Workshop on Cognitive Information Processing (CIP '08)*, Santorini, Greece, June 2008.